Phase diagram and transition temperatures in the system (T-T') La2-xNdxCuO4 ($x \leq 0.5$)

Mohamed Ikbal Houchati, Adnene Midouni, Mondher Yahya, Nassira Chniba-Boudjada, Jean-François Bardeau, Ahmed Hichem Hamzaoui

Phase diagram and transition temperatures in the system (T-T') $La_{2-x}Nd_xCuO_4$ ($x \leq 0.5$)

Mohamed Ikbal Houchati [a,b,c,*], Adnene Midouni [a], Mondher Yahya [a], Nassira Chniba-Boudjada [d], Jean-François Bardeau [e], Ahmed Hichem Hamzaoui [a]

[a] Laboratoire de Valorisation des Matériaux Utiles, Centre National des Recherches en Sciences des Matériaux, Technopôle Borj Cedria, B.P. 73, 8027 Soliman, Tunisie [b] Laboratoire de Recherche Catalyse et Matériaux pour l'Environnement et les Procédés CMEPRL (LR19ES08), Faculté des Sciences de Gabès/Université de Gabès, Campus Universitaire Cité Erriadh, Gabès 6072, Tunisie

[c] Institut de Chimie Moléculaire et des Matériaux-UMR 5253, C2M: Chimie et Crystallochimie des Matériaux, Université de Montpellier 2, 5 Place Eugène Bataillon, Bat 15, CC1504, F-34095 Montpellier, France

[d] Laboratoire de Cristallographie, CNRS, 25 Avenue des Martyrs, BP 166, 3804 Grenoble Cedex 9, France

[e] Institut des Molécules et Matériaux du Mans UMR CNRS 6283, Faculté des Sciences/Le Mans Université, Avenue Olivier Messiaen, 72085 Le Mans Cedex 9, France

ARTICLE INFO

Keywords:
Topotactic reaction
Temperature-dependent powder X-ray diffraction
Phase transition
Calcium hydride
EPR spectroscopy
Raman spectroscopy

ABSTRACT

$La_{2-x}Nd_xCuO_{3.5}$ ($x \leq 0.5$) compounds have been synthesized by a topotactic reduction reaction with calcium hydride at 280 °C for 48 h. Structural, thermal, vibrational and magnetic properties of $La_{2-x}Nd_xCuO_{3.5}$ ($x \leq 0.5$) were studied by X-ray powder diffraction (XRD), by differential thermal analysis (DTA) and temperature dependent powder X ray diffraction (TDXD), by Raman spectroscopy and by electronic paramagnetic resonance. The oxidation of the compounds $La_{2-x}Nd_xCuO_{3.5}$ ($x \leq 0.5$) at 400 °C for 24 h kinetically stabilizes the compounds $La_{2-x}Nd_xCuO_4$ ($x \leq 0.5$) with an *I4/mmm* type structure. The phase relationship between T' and T, ensured at high temperature, was followed and discussed by thermal and structural analysis.

1. Introduction

Cuprates with the general formula Ln_2CuO_4 (Ln: lanthanide) crystallize according to two different structures depending on the size of the Ln^{3+} ion, namely K_2NiF_4 of type (T/O), itself designated by T (Ln = La), the other of type T'-(Nd_2CuO_4) [1]. Thanks to their physicochemical properties, these cuprates constitute a very interesting material. The appearance of superconducting behavior in these cuprates [2] is due to the mixed valence state of copper which can be achieved either by performing cationic substitutions or by modifying the anionic lattice [3–6]. Recently, Tsukada et al. [7] synthesized for the first time and successfully the T' $(La\text{-}Ln)_2CuO_4$ phase as a thin layer at a temperature of 600 °C using the molecular beam epitaxy method. In this context, research has then been deepened in order to understand whether the T' (La_2CuO_4) phase exists only in the form of a thin layer and what are the conditions of stability of this phase. The research works of Takayama Muromachi et al. [8] showed both the stability of the T' phase by the co-precipitation method at a temperature of 600 °C and the synthesis of the T'-$La_{1.8}Y_{0.2}CuO_4$ phase. The T'-La_2CuO_4 phase was obtained for the first time following a classical oxidation–reduction reaction [9], where the topotactic reduction under a hydrogen atmosphere of the T-La_2CuO_4 phase leads to the formation of the S phase. At moderate temperature, the oxidation of this phase gives rise to the T'-La_2CuO_4 phase. More recently, well crystallized samples of the T'-La_2CuO_4 phase have been successfully synthesized by Imai [10], at temperature as low as 350 °C and under a reducing atmosphere by direct precipitation of the mixture of molten KOH/NaOH salts. Since alkali metal hydroxides have relatively low melting points and dissolve metal oxides, direct reaction becomes possible at significant low temperatures. On the other hand, heating to the same temperature in air leads to the stabilization of the T-La_2CuO_4 phase. The reproducibility of these experiments is difficult and until today there is no other publication confirming this result.

In this context, we were interested in the synthesis of the T' phase via a series of topotactic reactions where the reduction of the T-$La_{2-x}Nd_xCuO_4$ ($x \leq 0.5$) phase by calcium hydride leads to the formation of an oxygen-deficient phase of the type $La_{2-x}Nd_xCuO_{3.5}$ ($x \leq 0.5$). This "pseudo-S" phase is then similar to the T' phase with oxygen vacancies in the CuO_2 plane [11]. at moderate temperature (400 °C), the

* Corresponding author at: Laboratoire de Valorisation des Matériaux Utiles, Centre National des Recherches en Sciences des Matériaux, Technopôle Borj Cedria, B. P. 73, 8027 Soliman, Tunisie

E-mail addresses: ikb_med@yahoo.fr, medikbel.houchati@fsg.rnu.tn (M.I. Houchati).

https://doi.org/10.1016/j.inoche.2021.108845

topotactic oxidation kinetically stabilizes the T'-$La_{2-x}Nd_xCuO_4$ phase. In mixed $La_{2-x}Nd_xCuO_4$ ($x \leq 0.5$) oxides, the progressive substitution of smaller ions for the lanthanide leads to the formation of two solid solutions, one of the T/O type for low values of ×, the other type T' [3]. The transition from T to T' phase in the $La_{2-x}Nd_xCuO_4$ system is obtained for a value of × > 0.5. On the basis of numerous studies carried out on the structural phases T, T/O and T', it has been shown that the transition from the T/O structure to the T' structure appears for a value of t less than 0.866 [12]. After twenty years of intense research on superconductors, we still cannot estimate the thermodynamically most stable phase between T and T' phase [13]. However, we do believe that the possibility to synthesize the T' phase can open up the possibility of testing superconducting behavior in cuprates. For example, the compound of the type T-$La_{2-x}Ce_xCuO_4$ ($x = 0.15$) is known until today as non-superconducting unlike that of the type T'-$Nd_{2-x}Ce_xCuO_4$ ($x = 0.15$) which is superconducting of type n [14].

So, in the present study, we are interested in investigating the thermal stability of the T' phase in the $La_{2-x}Nd_xCuO_4$ ($x \leq 0.5$) system in order to determine the phase diagram of these compounds. The study of thermal stability and phase transitions is carried out by differential thermal analysis (DTA) and temperature-dependent powder X-ray diffraction (TDXRD). The vibrational properties were followed by Raman spectroscopy. The analysis of the magnetic properties of the reduced phases is studied by electronic paramagnetic resonance (EPR).

2. Experimental section

The synthesis of the compounds of T ($La_{2-x}Nd_xCuO_4$ ($x \leq 0.5$)) phase is ensured by mixing La_2O_3, Nd_2O_3 and CuO (Aldrich 99.9 %), previously annealed at 900 °C for 12 h. The powders were mixed in stoichiometric amounts, finely ground in an agate mortar and then heated at 1000 °C. Once this operation is carried out, the calcined powder is ground until a very fine powder is obtained, then one gram pellets (Φ = 13 mm) are prepared under a pressure of 9.451 Atm (10 tones) and under vacuum for about five minutes. Once the pellets are prepared, they are heated at 1000 °C for 24 h. These steps are repeated twice. The pellets are then placed under vacuum for one hour to avoid any reaction with the oxygen in the air. The assessment reaction is as follows:

$$La_2O_3 + Nd_2O_3 + CuO \rightarrow La_{2-x}Nd_xCuO_4$$

The topotactic reduction of the compounds of the T ($La_{2-x}Nd_xCuO_4$ ($x \leq 0.5$)) phase via calcium hydride at 280 °C leads to the formation of a new $La_{2-x}Nd_xCuO_{3.5}$ ($x \leq 0.5$) phase deficient in oxygen. The principle of reduction is complicated because calcium hydride CaH_2 is very delicate to the oxygen in the air; transformation and formation of $Ca(OH)_2$ will occur from the first contact. For this reason, the work is carried out in a glove box under an argon atmosphere. To synthesize the oxygen-deficient compounds $La_{2-x}Nd_xCuO_{3.5}$ ($x \leq 0.5$), a small quantity of powder of the order of 1 g taken from the samples already synthesized, is mixed with a quantity of powder of CaH_2 according to the equation of the following reaction:

$$La_{2-x}Nd_xCuO_4 + ½\ CaH_2 \rightarrow La_{2-x}Nd_xCuO_{3,5} + ½\ CaO + ½\ H_2$$

During the reaction, the amount of CaH_2 is added in excess of the order of 2 % to ensure the total reduction of the phases. The mixture of powder of T-$La_{2-x}Nd_xCuO_4$ ($x \leq 0.5$) phase and CaH_2 is grounded and then pelletized to obtain small pellets of the order of 5 mm in diameter which will be placed in a sealed tube heated for 48 h at a temperature of 280 °C. Two days later, the obtained powder obtained is poured into a solution containing a 0.1 M mixture of NH_4Cl and methanol in order to remove traces of residual CaO and CaH_2. The final obtained powder obtained is dried for half an hour and the study by X-ray diffraction proves that the phase obtained is pure and very well crystallized.

The compounds of the T'-$La_{2-x}Nd_xCuO_4$ ($x \leq 0.5$) system are obtained after oxidation of the compounds of the $La_{2-x}Nd_xCuO_{3.5}$ ($x \leq 0.5$) phase at a temperature of 400 °C for 12 h.

The phases are identified by X-ray powder diffraction. The diffraction patterns were obtained at room temperature using a D8 Bruker Advance diffractometer equipped with a Cu anticathode (CuK_α λ = 1.54056 Å). Crystal structures were refined using the Rietveld method using the Fullprof program [15]. The background was estimated by a Legendre function, and the peak shapes were described by a pseudo Voigt-function.

The powder X-ray diffraction (XRD) diagrams of the "pseudo-S" $La_{2-x}Nd_xCuO_{3.5}$ ($x \leq 0.5$) phases were recorded at room temperature over an angular range between 10 and 80° with a step of 0.014° in 2θ.

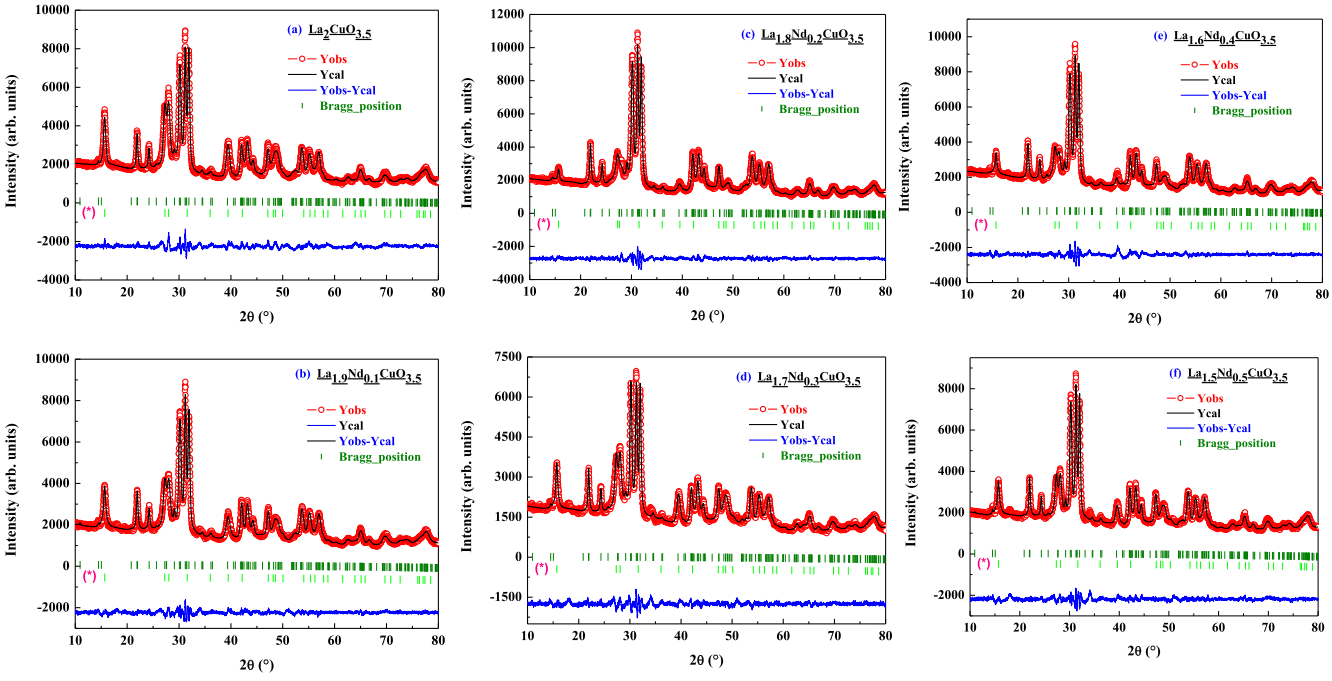

Fig. 1. Structural characterization by Rietveld refinement of X-ray powder diffraction data at room temperature of **(a)** $La_2CuO_{3.5}$, **(b)** $La_{1.9}Nd_{0.1}CuO_{3.5}$, **(c)** $La_{1.8}Nd_{0.2}CuO_{3.5}$, **(d)** $La_{1.7}Nd_{0.3}CuO_{3.5}$, **(e)** $La_{1.6}Nd_{0.4}CuO_{3.5}$ and **(f)** $La_{1.5}Nd_{0.5}CuO_{3.5}$.

Table 1
Structure data obtained from Rietveld refinement of XRD Powder Diffraction for compounds of the $La_{2-x}Nd_xCuO_{3.5}$ ($x \leq 0.5$) system. (Monoclinic symmetry and space group *A2/m*).

x		0.0	0.1	0.2	0.3	0.4	0.5
Phase		« Pseudo-S »					
Space group		A2/m					
a (Å)		8.6036(7)	8.5918(7)	8.5922(6)	8.6147(8)	8.5838(7)	8.5803(7)
b (Å)		3.8565(3)	3.8524(3)	3.8503(2)	3.8417(3)	3.8445(3)	3.8394(3)
c (Å)		13.0073(1)	12.9838(1)	12.9739(1)	12.9773(1)	12.9539(1)	12.9400(1)
β (°)		108.95(4)	108.93(6)	108.97(4)	109.06(7)	108.98(6)	109.02(6)
V (Å^3)		408.180	406.523	405.907	405.939	404.252	403.024
R_p		1.09	2.83	2.76	2.93	3.02	3.01
R_{wp}		1.41	3.60	3.46	3.77	4.03	3.93
χ^2		2.48	2.47	2.36	2.52	3.25	3.03
$La_{(1)}/Nd_{(1)}$	**x**	0.1630(9)	0.1659(8)	0.1641(6)	0.1627(1)	0.1599(6)	0.1645(9)
	y	0	0	0	0	0	0
	z	0.3538(8)	0.3459(4)	0.3453(3)	0.3426(5)	0.3502(3)	0.3440(5)
	Occ	2/0	1.9/0.1	1.8/0.2	1.7/0.3	1.6/0.4	1.5/0.5
$La_{(2)}/Nd_{(2)}$	**x**	0.3202(9)	0.3199(8)	0.3195(7)	0.3135(1)	0.3084(7)	0.3155(1)
	y	1/2	1/2	1/2	1/2	1/2	1/2
	z	0.1487(7)	0.1406(4)	0.1436(3)	0.1386(4)	0.1426(4)	0.1424(4)
	Occ	2/0	1.9/0.1	1.8/0.2	1.7/0.3	1.6/0.4	1.5/0.5
$Cu_{(1)}$	**x**	0	0	0	0	0	0
	y	0	0	0	0	0	0
	z	0	0	0	0	0	0
	Occ	1	1	1	1	1	1
$Cu_{(2)}$	**x**	1/2	1/2	1/2	1/2	1/2	1/2
	y	0	0	0	0	0	0
	z	0	0	0	0	0	0
	Occ	1	1	1	1	1	1
$O_{(1)}$	**x**	0	0	0	0	0	0
	y	1/2	1/2	1/2	1/2	1/2	1/2
	z	0	0	0	0	0	0
	Occ	1	1	1	1	1	1
$O_{(2)}$	**x**	0.2852(4)	0.2827(3)	0.2502(5)	0.2818(5)	0.2780(3)	0.2769(3)
	y	0	0	0	0	0	0
	z	0.0092(4)	−0.0258(2)	−0.0308(2)	−0.0098(4)	−0.0190(2)	−0.0298(2)
	Occ	2	2	2	2	2	2
$O_{(3)}$	**x**	0.3184(2)	0.3536(2)	0.3402(2)	0.2922(3)	0.3236(2)	0.3464(3)
	y	0	0	0	0	0	0
	z	0.8265(3)	0.8210(2)	0.8259(2)	0.7839(3)	0.7991(2)	0.8217(3)
	Occ	2	2	2	2	2	2
$O_{(4)}$	**x**	0.3706(7)	0.3812(5)	0.3780(5)	0.4243(5)	0.3868(5)	0.3906(5)
	y	0	0	0	0	0	0
	z	0.2436(1)	0.2462(1)	0.2354(1)	0.2546(2)	0.2374(1)	0.2423(1)
	Occ	2	2	2	2	2	2
$Cu_{(1)}$-$O_{(1)}$ (2x)		1.928	1.926	1.925	1.928	1.922	1.920
$Cu_{(1)}$-$O_{(2)}$ (2x)		2.418	2.557	2.311	2.472	2.477	2.528
$Cu_{(2)}$-$O_{(2)}$ (2x)		1.890	1.787	2.052	1.842	1.840	1.825
$La_{(1)}/Nd_{(1)}$-$O_{(3)}$		2.437	2.599	2.511	2.464	2.591	2.549
$La_{(2)}/Nd_{(2)}$-$O_{(3)}$		2.318	2.265	2.313	1.953	1.989	2.248
$La_{(2)}/Nd_{(2)}$-$O_{(4)}$ (2x)		2.254	2.324	2.233	2.435	2.262	2.287

Temperature-dependent X-ray diffraction (TDXRD) was performed using a powdered diffractometer, with $CuK_{\alpha 1}$ radiation $\lambda(K_{\alpha 1}) = 1.5406$ Å, selected with an incident beam quartz monochromator combining the INEL curve sensitive detector (CPS 120) and a high-temperature Rigaku attachment. These data were collected in air, with a heating rate of 10 °C/h from 450 to about 700 °C. Temperature calibration was performed with standard materials within the temperature range involved.

The powders were placed on a glass slide without any additional sample preparation; these samples were characterized by Raman analysis. The Raman measurements were performed at room temperature using a WITec Alpha 300R confocal Raman spectrometer (WITec GmbH, Ulm Germany) equipped with both a Ray Shield Coupler and a 1800 g. mm^{-1} grating blazed at 500 nm allowing spectra measurements at extremely low wave numbers and high spectral resolution (0.7 cm^{-1}). Raman spectra were recorded under a microscope, in the back scattering geometry, with a Zeiss EC Epiplan-Neofluar® 100 × objective (numerical aperture of 0.9) focusing the 532 nm line of a Solid State Sapphire laser (Coherent INC., Santa Clara, USA) on the samples. The laser power at the samples was kept at 0.2 mW in order to avoid sample degradation or heating. The Raman spectra were then systematically recorded 6 times in the wave number 25–1200 cm^{-1} region with an integration time of 600 s and finally averaged to improve the signal-to-noise ratio.

For the differential thermal analysis, the "Adamel ATD 67" analyzer was used with a heating rate of 10 °C/min in the temperature range [20–650 °C].

The EPR measurements were carried out with a Bruker ER-200D spectrometer operating in X-band. To obtain the resonance condition, the measurements are carried out at constant frequency while varying the magnetic field. The EPR spectra were recorded at room temperature and the static magnetic field was swept in the 2500–4500 Gauss range. Before any analysis, the samples were heated at 150 °C for 12 h, and the EPR tubes must be degassed to prevent the presence of residual water vapors which would distort the analysis. The sample in a powder form with a mass of 30 mg having paramagnetic centers, is introduced into an EPR tube and then placed in a cavity located in the center of a magnetic field of constant standard, intended to remove the degeneration of the electronic levels by the Zeeman effect. In practice, in an EPR experiment, the signal obtained is proportional to the number of spins participating in the resonance. However, the transition energy is too low to be directly exploited. To get around this drawback, the recorded signal corresponds

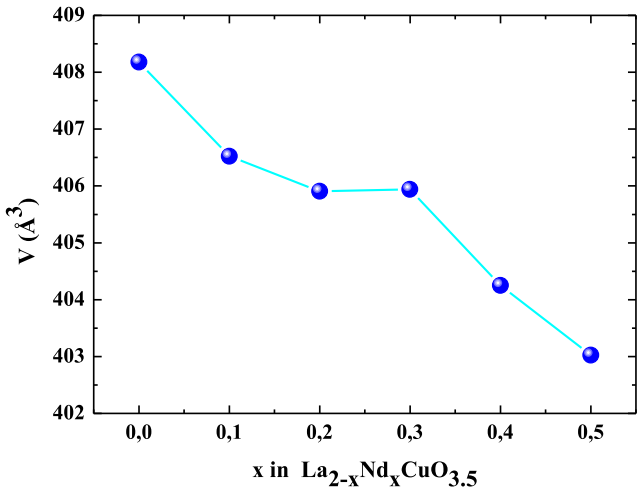

Fig. 2. Study of the variation of the cell volume compared to the neodymium composition of the compounds of the $La_{2-x}Nd_xCuO_{3.5}$ ($x \leq 0.5$) system.

to the first derivative of the absorption curve of the microwave wave with respect to the applied magnetic field.

3. Results and discussions

The topotactic reduction of the oxides of the T-$La_{2-x}Nd_xCuO_4$ ($x \leq 0.5$) phase at low temperature allows the kinetic stabilization of new phases $La_{2-x}Nd_xCuO_{3.5}$ ($x \leq 0.5$) with a rare and unprecedented coordination of copper. So, to synthesize this phase, calcium hydride was used as a reducing agent. The powder X-ray diffraction (XRD) diagrams of the "pseudo-S" $La_{2-x}Nd_xCuO_{3.5}$ ($x \leq 0.5$) phases were recorded at room temperature. The set of intense DRX diagram reflections can be indexed in the monoclinic cell of space group *A2/m*. The observed and calculated diagrams obtained after refinement are presented in the Fig. 1. An excellent agreement is obtained between the calculated profile and the experimental points by considering the space group *A2/m*. The atomic positions resulting from the refinement are presented in Table 1. Trace of $La(OH)_3$ can nevertheless be detected in final product. The presence of minor peaks in the pattern (indicated with *) is related this second minority phase. This result is in agreement with the literature [16–18] and the effect on the stoichiometry of the material is negligible. The transition from the orthorhombic to the monoclinic structure is achieved by replacing the CuO_6 octahedra by CuO_4 square planes and the $(La/Nd)O_9$ by the $(La/Nd)O_7$ polyhedra. The reduction of Cu^{2+} to Cu^{+} is accompanied by a decrease in the number of oxygen ligands which implies a change in the coordination of all the Cu and La(Nd) atoms. Indeed, the coordination of Cu goes from 6 to 4 and the octahedron of Cu is reduced to a square plane of oxygen and the coordination of La(Nd) goes from 9 to 7. Copper atoms have two states of mixed valence $Cu^{+/2+}$ ($3d^{10}/3d^{9}$) in such a way as to preserve the electroneutrality of the system. We thus obtain the compound of formula: $La^{3+}_{2-x}Nd^{3+}_{x}Cu^{+}_{y}Cu^{2+}_{z}O^{2-}_{3.5}$ ($y + 2z = 1$ ($z<0.5$)).

The a, b and c lattice parameters in the compounds of the $La_{2-x}Nd_xCuO_{3.5}$ ($x \leq 0.5$) system decrease with increasing proportion of neodymium. Fig. 2 shows the evolution of cell volume as function of the composition i.e. the proportion neodymium.

Electronic Paramagnetic Resonance (EPR) is presented as a technique allowing the study of the environment of species having one or more unpaired electrons, particularly for ions of transition metals such as copper, which is the subject of our study. In the stoichiometric La_2CuO_4 and $La_{2-x}M_xCuO_4$ (M: isovalent cation of lanthanum atoms, such as Nd^{3+}, Pr^{3+}), all copper are divalent (formula with oxidation numbers $La^{3+}_{2-x}M^{3+}_{x}Cu^{2+}O^{2-}_{4}$). Cu^{2+} is a d^9 metal ion and is readily observable by EPR. The compounds $La_{2-x}Nd_xCuO_{3.5}$ are obtained by

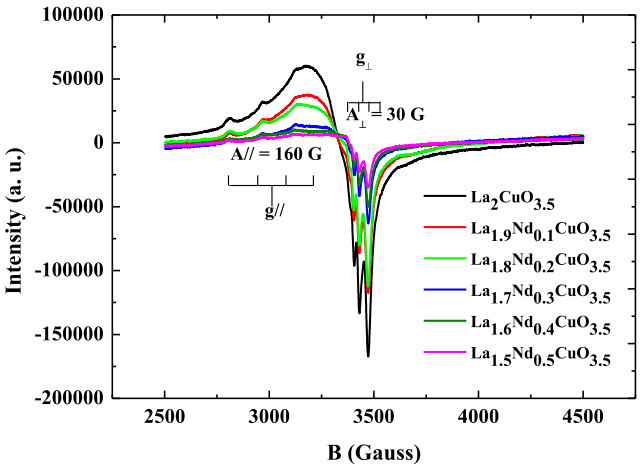

Fig. 3. EPR spectra of the compounds $La_{2-x}Nd_xCuO_{3.5}$ ($x \leq 0.5$).

reduction of all the Cu^{2+} ions to Cu^{+} species (formula with oxidation numbers $La^{3+}_{2-x}M^{3+}_{x}Cu^{1+}O^{2-}_{3.5}$). Cu^{+} with a d^{10} electronic configuration it is diamagnetic and cannot be seen in EPR.

The X-band EPR spectra of $La_{2-x}Nd_xCuO_{3.5}$ at several × values between 0 and 0.5 recorded at room temperature show a signal characteristic of the Cu^{2+} ion (Fig. 3). The entity observed after reduction is therefore still unreduced Cu^{2+}. Existence of Cu^{2+} ions shows that the reduction is not total, and the compounds $La_{2-x}Nd_xCuO_{3.5}$ are not stoichiometric. Thus, the real formula is $La_{2-x}Nd_xCuO_{3.5+\delta}$, with a detailed formula $La^{3+}_{2-x}Nd^{3+}_{x}Cu^{+}_{1-2\delta}Cu^{2+}_{2\delta}O^{2-}_{3.5+\delta}$. The apparent excess of oxygen in the chemical formula is due to interstitial oxygen, or to cationic vacancies with oxygen stoichiometry remains intact.

On the other hand, the signal has a hyperfine structure comprises four lines ($2I + 1$ with $I = 3/2$) is characteristic of Cu^{2+} ions isolated in axial symmetry. This signal has parallel and perpendicular components. Considering that Oz is the axis of symmetry, the absorption spectrum has two maxima corresponding to $g_z = g_{//}$ and $g_x = g_y = g_{\perp}$, and $g_{//} > g_{\perp} > 2$, indicating a tetragonal distortion with elongation at the z axis. These EPR parameters $g_{//}$ and $g_{\perp}$ depend on the nature of the bonds which surround the Cu^{2+} ions in a given symmetry. Copper has two stable isotopes, ^{63}Cu and ^{65}Cu, with relative abundances of 69.15 % and 30.85 %, respectively. Each having a nuclear spin $I = 3/2$. An interaction between it and the electron spin is possible. This is consistent with the relation $2(2I + 1)$ components which can be observed. Each electron spin sublevel will be broken down into $2I + 1$ nuclear sublevel. The $^{63,65}Cu^{2+}$ ion has an electron spin $S = 1/2$ and a nuclear spin $I = 3/2$. In the case of a hyperfine structure, eight lines will be observed [19].

In the recorded spectra, four equally spaced EPR peaks are observed at low magnetic field, in addition, four EPR peaks are observed at a higher magnetic field. They are attributed to the hyperfine structure signals. Apparently, the responses of both $^{63}Cu^{2+}$ and $^{65}Cu^{2+}$ are merged into a single peak broad. The EPR signal is thus formed from two series of four lines (parallel and perpendicular components). The perpendicular components in the high field region are well resolved, and it can be observed that the spectrum high field side is more intense than the low field side. Moreover, the hyperfine structure with increasing amplitude for the components towards higher magnetic fields is characteristic of Cu^{2+} centers in a distorted octahedral site undergoing Jahn–Teller distortion and are explained by the 'rapid tumbling motion' effect [20]. Except intensity all EPR parameters are identical regardless of the substitution rate (x). The parameters EPR are: $g_{//} = 2{,}306$; $g_{\perp} = 2{,}056$; ($g_{iso} = \frac{1}{3}(g_{//} + 2\,g_{\perp}) = 2{,}139$). The hyperfine coupling constants (components A) determined from the separation between two consecutive lines of the hyperfine structure are: $A_{//} = 160$ G and $A_{\perp} = 30$ G ($A_{iso} = \frac{1}{3}(A_{//} + 2\,A_{\perp}) = 73$ G). These parameters characterize isolated Cu^{2+} ions, in axial

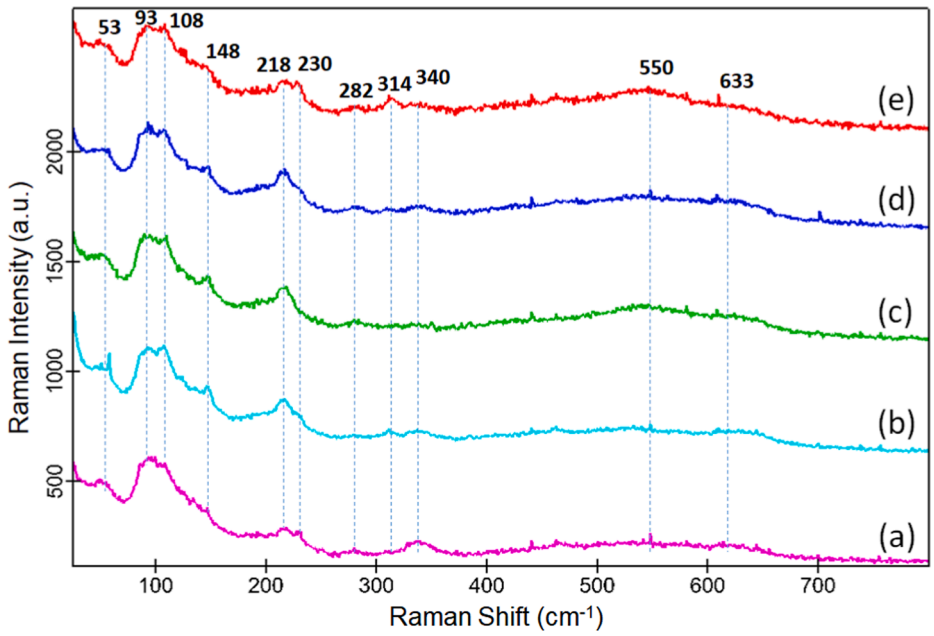

Fig. 4. Ramans spectra of **(a)** $La_{1.9}Nd_{0.1}CuO_{3.5}$, **(b)** $La_{1.8}Nd_{0.2}CuO_{3.5}$, **(c)** $La_{1.7}Nd_{0.3}CuO_{3.5}$, **(d)** $La_{1.6}Nd_{0.4}CuO_{3.5}$ and **(e)** $La_{1.5}Nd_{0.5}CuO_{3.5}$.

symmetry. In addition, these results clearly show that the Cu^{2+} ions present in these solids keep the same environment [19].

The changes observed in the EPR line intensities could be attributed to either:

- The change in the content of paramagnetic center Cu^{2+}. Which results in the change in the deviation from stoichiometry (δ) with, number of Cu^{2+} is equal to 2δ.
- Or to what is called the "skin effect". According to this effect, the value of the sample which could be penetrated by microwave radiation decreases as the conductivity increases [21]. In this case the electrical conductivity increases with the percentage of substitution at La-ions site.
- In addition, the increase in the amount of copper in these samples can lead to the formation of agglomerates not detectable in RPE as due to the presence of strang short range antiferromagnetic interactions between sufficiently close Cu^{2+} ions, with contributes to the decrease in the intensity of signal relating to the isolated Cu^{2+} ions [22–23].

From these observations, we can say that there is simultaneous presence of two species Cu^{2+} and Cu^{+} whatever the value of x. the Cu^{2+}

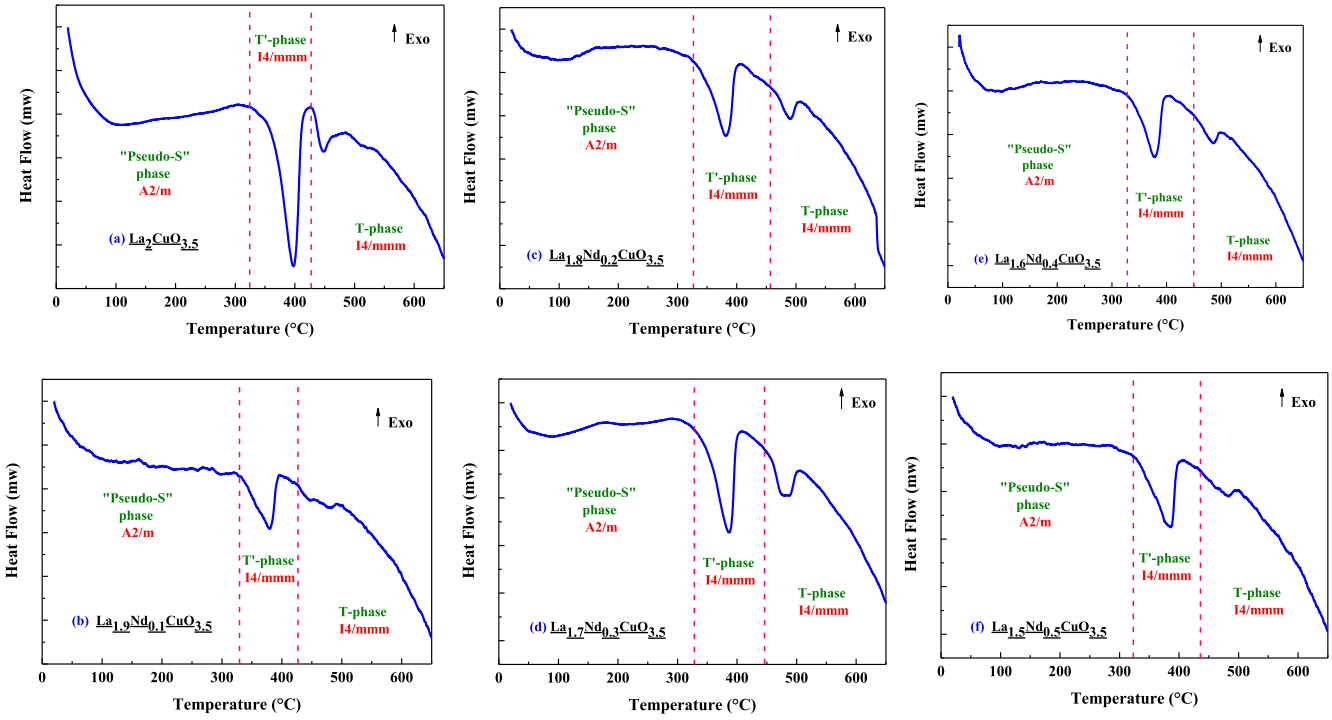

Fig. 5. Differential thermal analysis (DTA) of **(a)** $La_2CuO_{3.5}$, **(b)** $La_{1.9}Nd_{0.1}CuO_{3.5}$, **(c)** $La_{1.8}Nd_{0.2}CuO_{3.5}$, **(d)** $La_{1.7}Nd_{0.3}CuO_{3.5}$, **(e)** $La_{1.6}Nd_{0.4}CuO_{3.5}$ and **(f)** $La_{1.5}Nd_{0.5}CuO_{3.5}$.

ions occupy the same type of site.

In the literature, La_2CuO_4 [24] presents a prototype compound which shows a change in the Raman spectrum due to the existence of a polymorphism. With temperature or under pressure, the structural phase transitions modify the number of vibrational modes at the zone center. At high temperature, the structure of La_2CuO_4 is tetragonal of the K_2NiF_4 type (crystallographic space group *I4/mmm* or D_{4h}^{17}); below ≈ 500 K, the structure deforms into an orthorhombic structure (*Pmmm* or D_{2h}^{18}). Theoretical analysis of the vibrational modes of the tetragonal structure gives $2A_{1g} + 2E_g$ Raman active modes and $3A_{2u} + 4E_u$ IR active modes and a silent B_{2u} mode [25–28]. The Fig. 4 shows the Raman spectra of the $La_{2-x}Nd_xCuO_{3.5}$ ($x \leq 0.5$) compounds recorded at room temperature.

The spectra show more peaks than expected from the selection rules suggesting that the crystal structure is of lower symmetry. Although the spectra are complicated and difficult to fully explain, three main domains can nevertheless be observed below 400 cm^{-1}. The broad band between 70 and 170 cm^{-1}, composed of two intense peaks at 98 and 108 cm^{-1}, can be attributed to the rotational mode of the CuO_6 octahedra. The small intensity band at 148 cm^{-1} can be assigned to the vibration of La atom along the × axis and the broad brand between 200 and 240 cm^{-1}, can be attributed to the vibrations of La atoms along the z axis [29]. Accordingly, the bands we observed for $La_{2-x}Nd_xCuO_4$ are similar to the bands reported at 118, 147 and 223 cm^{-1} by Lin et al. [30] for $La_{1.9}Sr_{0.1}CuO_4$. We noticed that the band, attributed to the axial breathing of the octahedral, usually observed around 426 cm^{-1} for La_2CuO_4 [31] is not observed in the Raman spectra, confirming what has already been reported when La atom is substituted by another atom. Moreover, with substitution of Nd for La, it is possible that forbidden modes (infrared-active modes) appear in the Raman spectra by the break of symmetry. In that case, it could explain the appearance of bands with small intensity located at approximatively 282, 314, and 340 cm^{-1} in the Raman spectra. Finally, two-phonon scattering can be observed in the 400–700 cm^{-1} region where broad bands can be detected. In the case of La_2CuO_4 [30] strong intensity bands are commonly reported in this specific region and the bands are then assigned to the contribution of infrared-active phonons to the Brillouin zone center. With the doping these strong bands are reduced and residual broad bands participate in modifying the intensity of Raman spectra recorded in this region.

The Fig. 5 show the results of the differential thermal analysis of the compounds of the $La_{2-x}Nd_xCuO_{3.5}$ ($x \leq 0.5$) system. Based on these studies, it is possible to determine and verify the existence of the structural change following the oxidation of these phases under a nitrogen flow rate of the order of 10 ml/min and via increasing the temperature by 20 up to at 650 °C with a heating rate of the order of 10 °C/min. Two endothermic inflection points are shown in the curves after study; the first peak is located in the temperature range ~ 320–420 °C. It is explained by a first transition: from the "pseudo-S" to the T'-$La_{2-x}Nd_xCuO_4$ ($x \leq 0.5$) phase from temperature 320 °C. The second endothermic peak obtained at high temperature (T > 450 °C) shows the thermal stabilization of the T-$La_{2-x}Nd_xCuO_4$ phase ($x \leq 0.5$) which crystallizes at high temperature in a tetragonal lattice *I4/mmm*.

To check them, isothermal oxidation was carried out for the reduced $La_{2-x}Nd_xCuO_{3.5}$ ($x \leq 0.5$) phases at 400 °C and then at a temperature above 500 °C, hence explaining the existence of these two peaks.

X-ray diffraction analysis, on a Bruker D8 advance diffractometer, compounds oxidized at T = 400 °C are shown in the Figure. S1. The cell parameters are refined using the Rietveld method implemented in the Fullprof software [15].The powder diffractograms were recorded with a counting step of 0.014° (2θ). The space group retained is *I4/mmm* similar to that of the T' of Nd_2CuO_4 phase. The agreement obtained between the calculated and experimental crystallographic data is satisfactory with reasonable parameters. The results of the structural refinement are summarized in the Table. S1. Based on the results obtained, we notice the adjustment between the observed and calculated

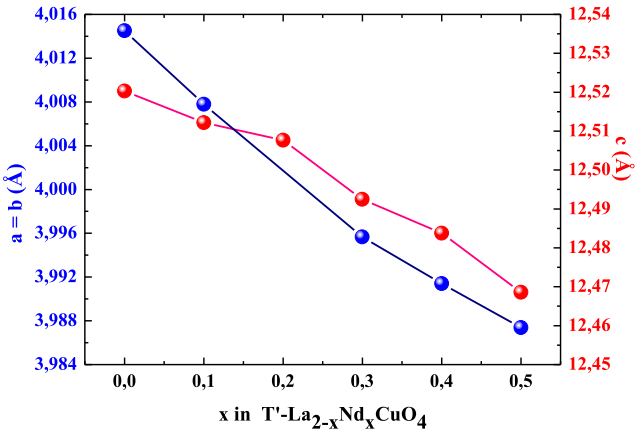

Fig. 6. Study of the variation of the cell parameters a, b and c with respect to the neodymium composition of the compounds of the T'-$La_{2-x}Nd_xCuO_4$ ($x \leq 0.5$) system.

Table 2
Study of the temperature variation from the T'-$La_{2-x}Nd_xCuO_4$ to the T-$La_{2-x}Nd_xCuO_4$ ($x \leq 0.5$) phase with respect to the neodymium composition.

Compounds	Transition temperature (°C)
T'-La_2CuO_4 → T-La_2CuO_4	515
T'-$La_{1.9}Nd_{0.1}CuO_4$ → T-$La_{1.9}Nd_{0.1}CuO_4$	580
T'-$La_{1.8}Nd_{0.2}CuO_4$ → T-$La_{1.8}Nd_{0.2}CuO_4$	645
T'-$La_{1.7}Nd_{0.3}CuO_4$ → T-$La_{1.7}Nd_{0.3}CuO_4$	655
T'-$La_{1.6}Nd_{0.4}CuO_4$ → T-$La_{1.6}Nd_{0.4}CuO_4$	666
T'-$La_{1.5}Nd_{0.5}CuO_4$ → T-$La_{1.5}Nd_{0.5}CuO_4$	673

diagrams, and we can therefore deduce the structures of the T'-$La_{2-x}Nd_xCuO_4$ ($x \leq 0.5$) phases. The synthesis of T' phase, synthesized for the first time as a thin layer [7], via a series of topotactic reactions using a conventional reduction–oxidation reaction and based on a hydride of electropositive metals such as CaH_2, is currently of significant technological interest in the preparation of new superconducting compounds. Indeed, the question that arises can only be located at the level of thermodynamic stability. This question revolves around which phase could be the most thermodynamically stable; is it T or T' phase? The answer to this question, after several years of intense research on this type of compound, remains unanswered until now.

The oxygen atoms in the T'-phase structure are shifted away from Cu atoms to form lines of oxygen atoms along the c axis perpendicular to the CuO_2 planes. The sequence of atomic planes along the c axis is: CuO_2 and La(Nd)–O_2-(Nd)La. The Cu^{2+} cation is surrounded by four oxygen atoms forming a square plane. The cation $La(Nd)^{3+}$ has a coordinence of 8. The increase in the composition of neodymium in the compounds of the T'-$La_{2-x}Nd_xCuO_4$ ($x \leq 0.5$) structurally presents a decrease in cell parameters a, b and c as mentioned in the Fig. 6. The bonds lengths of La-$O_{(2)}$ and Cu-$O_{(1)}$ vary from 2.378 to 2.360 and from 2.004 to 1.995, respectively (Table. S1). Thus showing a decrease with increasing composition of neodymium.

Figures S2 show a temperature-dependent X-ray diffraction (TDXRD) study of all T'-$La_{2-x}Nd_xCuO_4$ ($x \leq 0.5$) compounds. The analysis of this study shows the existence of a phase transition to a temperature above 500 °C, the same result as that obtained by by Differential Thermal Analysis (DTA). The interpretation of the high-temperature transition is explained by a transition from the T' to the T phase. The Table. 2 summarizes the different temperatures of transitions from T' to T phase depending on the composition of neodymium (x). The Figure. S3 present variation in the composition of neodymium according to temperature. The interpretation of this variation shows that the transition temperature from T' to T phase increases with the increase in neodymium composition. The change in the cell volume of the compounds in the T'-

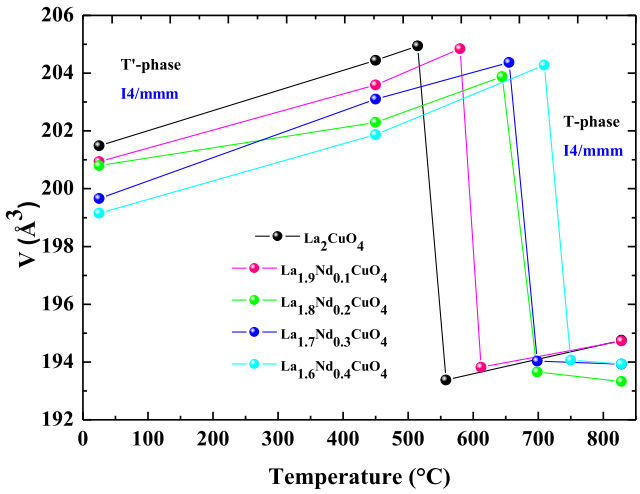

Fig. 7. Study of the variation of the cell volume respect to the temperature for the compounds of the T'-$La_{2-x}Nd_xCuO_4$ ($x \leq 0.5$) system.

$La_{2-x}Nd_xCuO_4$ ($x \leq 0.5$) according to temperature is shown in the Fig. 7. Based on this result, the transition from T' to T phase is assured for a critical volume of around 205 $Å^3$. Therefore, the increase in neodymium composition in the compounds of the T'-$La_{2-x}Nd_xCuO_4$ ($x \leq 0.5$) results in a clear decrease in cell parameters and thus a decrease in volume. Consequently, the transition from T' to T phase requires more energy, thus requiring a higher temperature up to a critical volume to stabilize the T-phase structure (*I4/mmm*) at high temperature.

Based on the results of the temperature-dependent X-ray diffraction (TDXRD) study, samples from the T-$La_{2-x}Nd_xCuO_4$ ($x \leq 0.5$) phases were obtained at a temperature above 500 °C following heating of the T'-$La_{2-x}Nd_xCuO_4$ phases ($x \leq 0.5$). The transition temperature from T' to T phase varies and increases with the increase in neodymium composition. The X-ray analysis study on a D8 Advance diffractometer of samples from the T-$La_{2-x}Nd_xCuO_4$ ($x \leq 0.5$) phases obtained after heating to the temperature of 900 °C of the T'-phases, gives us the diagrams depicted in the Figure. S4. The powder diffractograms of the T-$La_{2-x}Nd_xCuO_4$ ($x \leq 0.3$) phases are recorded with a counting step of 0.014° (2θ). The selected space group is *Bmab*, corresponding to that of T of La_2CuO_4 phase. The calculated and experimental crystallographic data, which is reasonably set up, agree. The results of the structural refinement are summarized in the Table. S2. The structure is described by stacking CuO_2-type leaflets separated between them by double layers of NaCl type along the c-axis. The coordinence of the lanthanum atom is equal to 9. That is 4 + 4 + 1 ions of oxygen with different binding lengths. The Cu transition metal is in coordinence 4 in relation to equatorial oxygen and 2 in relation to apical oxygen. In the $0.40 \leq x \leq 0.50$ composition domains, the two solid T/O and T' solutions coexist. The formation of a new structure T'', very close to T', and in which there would be an order between the ions La^{3+} and Nd^{3+} was proposed by J.B. Goodenough et al. [32].

4. Conclusion

We have shown topotactic reduction of the transition metal complex T-$La_{2-x}Nd_xCuO_4$ ($x \leq 0.5$) kinetically stabilizes new phases of deficient anions with unique transition oxygen metal $La_{2-x}Nd_xCuO_{3.5}$ ($x \leq 0.5$). The copper transition metal in the "pseudo-S" phase has a mixed valence $Cu^{+}/^{2+}$ ($3d^{10/9}$) explaining the existence of paramagnetic behavior in this type of materials. Thermal analyses of the compounds of the $La_{2-x}Nd_xCuO_{3.5}$ ($x \leq 0.5$) system show the existence of two phase transitions. The transition from T' to T phase observed at high temperatures increases with the increase in neodymium composition in T'-$La_{2-x}Nd_xCuO_4$ ($x \leq 0.5$). Topochemical manipulation at low temperature of complex oxides, whether by deintercalation of reducing anions or an oxidizing anion insertion, offers many possibilities for the synthesis of a wide range of new, metastable materials that could be used for solid oxide fuel cells. New low-temperature reactions offer the prospect of being able to synthesize the desired solid phases on demand to study superconductivity in this type of T'-T ($La_{2-x}Nd_xCuO_4$ ($x \leq 0.5$)) materials.

Declaration of Competing Interest

The authors declare that they have no known competing financial interests or personal relationships that could have appeared to influence the work reported in this paper.

Appendix A. Supplementary material

Supplementary data to this article can be found online at https://doi.org/10.1016/j.inoche.2021.108845.

References

[1] K. Zhenga, A. Gorzkowska-Sobaś, K. Świerczek, Evaluation of Ln_2CuO_4 (Ln: La, Pr, Nd) oxides as cathode materials for IT-SOFCs, Mater. Res. Bull. 47 (2012) 4089–4095, https://doi.org/10.1016/j.materresbull.2012.08.072.
[2] K. M. Shen, J. C. S. Davis, Cuprate high-TC superconductors, materialstoday 11 (2008) 14–21. https://doi.org/10.1016/S1369-7021(08)70175-5.
[3] C. Rial, E. Morán, M. A. Alario-Franco, U. Amador, N.H. Andersen, Structural and superconducting properties of La2−xNdxCuO4+y ($0 \leq x \leq 0.5$) prepared by room temperature chemical oxidation, Physica C: Superconductivity, 282 (1997) 781–782. https://doi.org/10.1016/S0921-4534(97)00410-3.
[4] F. Arrouy, A. Wattiaux, C. Cros, G. Demazeau, J-C. Grenier, M. Pouchard, J. Etourneau, Superconducting behaviour of the T/O structural type phase La2-xNdxCuO4+δ ($0 < x < 0.60$) under oxidizing conditions, Physica C 175 (1991) 342–346. https://doi.org/10.1016/0921-4534(91)90607-Z.
[5] C. Rial, E. Morán, M.A. Alario-Franco, U. Amador, N.H. Andersen, Structure and superconductivity of room temperature chemically oxidized La2-xNdxCuO4+y ($0 \leq x \leq 0.5$), Physica C 288 (1997) 91–104. DOI:10.1016/s0921-4534(97)01562-1.
[6] F. Arrouy, A. Wattiaux, E. Marquestaut, C. Cros, G. Demazeau, J.C. Grenier, M. Pouchard, Superconductivity in the La_2CuO_4-Nd_2CuO_4 system after treatment under oxidizing conditions, J. Solid State Chem. 115 (1995) 540–548, https://doi.org/10.1006/jssc.1995.1171.
[7] A. Tsukada, Y. Krockenberger, M. Noda, H. Yamamoto, D. Manske, L. Alff, M. Naito, New class of T'-structure cuprate superconductors, Solid State Commun. 133 (2005) 427–431, https://doi.org/10.1016/j.ssc.2004.12.011.
[8] E. Takayama-Muromachi, Y. Uchida, K. Kato, Electron-doped system (La, Nd, Ce)$_2$CuO$_4$ and preparation of T′-type (La, Ln)CuO$_4$ (Ln = Ce, Y), Physica C 165 (1990) 147–151, https://doi.org/10.1016/0921-4534(90)90159-C.
[9] F.C. Chou, J.H. Cho, L.L. Miller, D.C. Johnston, New phases induced by hydrogen reduction and by subsequent oxidation of L_2CuO_4 (L = La, Pr, Nd, Sm, Eu, Gd), Phys. ReV. B 42 (1990) 6172–6180, https://doi.org/10.1103/PhysRevB.42.6172.
[10] Y. Imai, M. Kato, Y. Takarabe, T. Noji, Y. Koike, Low-temperature synthesis of La_2CuO_4 with the T'-structure from molten hydroxides, Chem. Mater. 19 (2007) 3584–3585, https://doi.org/10.1021/cm070203n.
[11] M.I. Houchati, N. Chniba-Boudjada, A.H. Hamzaoui, Investigations on synthesis and electrical properties of the $La_{1.75}Nd_{0.1}Ce_{0.15}CuO_{3.5}$ prepared by topotactic reduction with CaH_2, J. Coord. Chem. 73 (2020) 1881–1894, https://doi.org/10.1080/00958972.2020.1799994.
[12] J. Hadermann, G. Van Tendeloo, HREM study of fluorinated Nd_2CuO_4, J. Solid State Chem. 157 (2001) 56–61, https://doi.org/10.1006/jssc.2000.9038.
[13] B. Marzougui, M.I. Houchati, Y. Ben Smida, N. Chniba-Boudjada, A.H. Hamzaoui, Topotactic transformation of (T-T')La1.8Nd0.2CuO4: Synthesis, structure, electrical properties and oxygen diffusion pathways simulation, Int. J. Hydrogen Energy In Press, Corrected Proof.
[14] Q. Liu, Z. Xiao, H. Xie, J. Gao, M. Yuan, W. Dong, Multifunctional layer-perovskite oxide $La_{2-x}Ce_xCuO_4$ for solid oxide fuel cell applications, Int. J. Hydrogen Energy 46 (2021) 9818–9825, https://doi.org/10.1016/j.ijhydene.2020.06.063.
[15] H.M. Rietveld, Line profiles of neutron powder-diffraction peaks for structure refinement, Acta crystallographica Acta crystallographica 22 (1967) 151–152, https://doi.org/10.1107/S0365110X67000234.
[16] M.I. Houchati, M. Ceretti, C. Ritter, W. Paulus, From T to T′-La_2CuO_4 via Oxygen Vacancy Ordered $La_2CuO_{3.5}$, Chem. Mater. 24 (2012) 3811–3815, https://doi.org/10.1021/cm302485q.
[17] M.I. Houchati, I. Houchati, A. Midouni, M. Ceretti, A.H. Hamzaoui, W. Paulus, Topotactic reduction and phase transitions in (T, T′) $L_{a1.8}P_{r0.2}Cu_O4$, Arabian J. Chem. 10 (2017) S3792–S3797, https://doi.org/10.1016/j.arabjc.2014.05.015.
[18] A. Midouni, M.I. Houchati, W.B.H. Othmen, N. Chniba-Boudjada, A.H. Hamzaoui, Topochemical reduction of the oxygen-deficient Ruddlesden−Popper phase (n = 1) $La_{1.85}Ca_{0.15}CuO_{4-\delta}$ and electrical properties of the $La_{1.85}Ca_{0.15}CuO_{3.5}$, Arabian J. Chem. 12 (2019) 4377–4387, https://doi.org/10.1016/j.arabjc.2016.06.006.

[19] A. Punnoose, R.J. Singh, EPR studies of high-TC superconductors and related systems, Int. J. Mod Phys B 9 (1995) 1123–1157, https://doi.org/10.1142/S0217979295000471.
[20] V.V.S.S. Sai Sundar, A. Karthikeyani, R. Jagannathan, Structural distortion in (La, Sr)2Cu$_O$4 cuprates: an insight using luminescence and EPR probes, Chem. Phys. Lett. 301 (1999) 417–424, https://doi.org/10.1016/S0009-2614(99)00026-3.
[21] R.J. Singh, Model of Preformed Hole-Pairs in Cuprate Superconductors, J. Modern Phys. 2 (2011) 885–897, https://doi.org/10.4236/jmp.2011.28105.
[22] R. Janes, M.R. Little, M. Parker, N. Akhtar, An EPR study of Cu^{2+} substitution in La_2NiO_4, J. Magn. Magn. Mater. 136 (1994) L13–L17, https://doi.org/10.1016/0304-8853(94)90438-3.
[23] B.I. Kochelaev, G.B. Teitel'baum, Nanoscale Properties of Superconducting Cuprates Probed by the Electron Paramagnetic Resonance, Struct. Bond 114 (2005) 205–266, https://doi.org/10.1007/b101021.
[24] W.H. Weber, C.R. Peters, E.M. Logothetis, Raman studies of lanthanum cuprate superconductors, J. Opt. Soc. Am. B 6 (1989) 455–464, https://doi.org/10.1364/JOSAB.6.000455.
[25] C. Thomsen, Light scattering in high-*Tc* superconductors, in: M. Cardona, G. Güntherodt (Eds.), Light Scattering in Solids VI, Topics in Applied Physics 68, Springer, Berlin, Heidelberg, 1991, https://doi.org/10.1007/3540536140_22.
[26] G. Burns, G.V. Chandrashekhar, F.H. Dacol, M.W. Schafer, P. Strobel, Phonons in the high temperature $Bi_2Ca_{n-1}Sr_2Cu_nO_{4+2n}$ superconductors, Solid State Commun. 67 (1988) 603–607, https://doi.org/10.1016/0038-1098(88)90175-5.
[27] J.R. Ferraro, V.A. Maroni, The characterization of high-critical-temperature ceramic superconductors by vibrational spectroscopy, Appl. Spectrosc. 44 (1990) 351–366, https://doi.org/10.1366/0003702904086047.
[28] R. Feile, Lattice vibrations in high-Tc superconductors: Optical spectroscopy and lattice dynamics, Physica C 159 (1989) 1–32, https://doi.org/10.1016/0921-4534(89)90099-3.
[29] S. Sugai, Phonon Raman scattering in $(La_{1-x}Sr_x)_2CuO_4$ single crystals, Phys. Rev. B 39 (1988) 4306–4315, https://doi.org/10.1103/PhysRevB.39.4306.
[30] Y. Lin, J.E. Eldridge, J. Sichelschmidt, S.W. Cheong, T. Wahlbrink, Fröhlich-interaction induced one-phonon Raman scattering in La_2CuO_4 using an infrared laser, Solid State Commun. 112 (1999) 315–318, https://doi.org/10.1016/S0038-1098(99)00366-X.
[31] V.N. Denisov, B.N. Mavrin, V.B. Podobedov, A.B. Bykov, A.F. Goncharov, L. P. Zibrov, O.K. Mel'nikov, Raman scattering in $La_{2-x}Sr_xCuO_4$ single crystals, Phys. Lett. A 140 (1989) 141–146, https://doi.org/10.1016/0375-9601(89)90508-2.
[32] A. Manthiram, J.B. Goodenough, Thermal-expansion mismatch and intergrowth types in the system $La_{2-y}Nd_yCuO_4$, J. Solid State Chem. 92 (1991) 231–236, https://doi.org/10.1016/0022-4596(91)90262-G.